ISSN(Online): 2320 - 9801
ISSN (Print) : 2320 - 9798

International Journal of Innovative Research in Computer and Communication Engineering

(An ISO 3297: 2007 Certified Organization)

Vol. 4, Issue 6, June 2016

An Enhanced Framework for Change Detection in Very High Resolution Remote Sensing Images

Eng. Mostafa Mosaad [1], Dr. Fawzy Eltohamy[1], Dr.Mahmoud Safwat[2], Dr. Ashraf K. Helmy[3]

Department of Aircraft Electric Equipment, Military Technical College, Cairo, Egypt[1]

Department of Electrical Measurement, Military Technical College, Cairo, Egypt[2]

National Authority of Remote Sensing and Space Sciences, Cairo, Egypt[3]

ABSTRACT: Land-cover (LC) and land-use (LU) change information is important due to its practical uses in various applications. Increasing the geometrical resolution of remote sensing images makes the change detection (CD) process to be complicated. In this paper, An enhanced framework based on the spatial context information of multitemporal adaptive regions homogeneous both in spatial and temporal domain (parcels) is presented to detect the semantic changes in the very high resolution (VHR) remote sensing multitemporal images. The proposed framework uses the absolute difference between {red, green, blue and hue} layers instead of the use of change vector analysis proposed by Lorenzo Bruzzone and Francesca Bovolo in 2013. Two experiments are performed to test the performance of the proposed framework. The first experiment shows that the proposed framework gives 72.8 % CD accuracy while the published framework gives 18.69 %. The second experiment shows that the proposed framework gives 83 % overall accuracy, while the published framework gives 74 %. The results indicate that the proposed framework detects 18.16 % had been changed from the total area and the published framework gives 10.41%.

Keywords Change detection (CD), change vector analysis (CVA), multitemporal images, registration noise (RN), shadow index, very high resolution (VHR) images, IHS transformation.

I. INTRODUCTION

The earth surface is changing due to human activity or natural phenomena [1]. The remote sensing (RS) data has become a major source for CD studies because of its high temporal frequency, suitable digital format computation, synoptic view, and wider selection of spatial and spectral resolutions [2]. CD in remote sensing can be defined as ‘‘the process of identifying differences in the state of an object or phenomenon by observing it at different times’’ [3]. Due to the huge amount of data acquired from the satellite sensors, unsupervised change detection methods are required to extract the changes without relying on both the manual processing of experts and the availability of ground truth information [4]. A landmark review of the most commonly used methods for detecting changes was presented in [5], [6]. Generally these methods can be classified into two main categories: pre-classification and post-classification change detection methods [7]**.** However, these methods are ineffective when dealing with very high geometrical resolution (metric or submetric) [8]. As, increasing the geometrical resolution results in the possibility of identifying much more details which make the assumption of spatial independence among pixels is not reasonable [9].

Most reviews assume that the similarity in radiometric properties in dataset except for the presence of changes occurred on the ground especially after preprocessing procedures [10]. This assumption is seldom satisfied in VHR images during the presence of false changes such as shadow and registration noise [8]. This makes the change detection task more complex. Respectable attempts try to solve this problem by detecting the changes as in [11], [12], [13], [14]. All these attempts don’t reveal the false changes like shadow and registration noise. In this paper, a general framework based on context sensitive analysis is presented to reduce the impact of shadow and registration noises that impose themselves in the change detection process especially for VHR images.

This paper is organized in five sections. The next section recalls related work. The third section illustrates the general framework for detecting the semantic changes in the VHR images. The fourth section describes the

ISSN(Online): 2320 - 9801
ISSN (Print) : 2320 - 9798

International Journal of Innovative Research in Computer and Communication Engineering

(An ISO 3297: 2007 Certified Organization)

Vol. 4, Issue 6, June 2016

experimental work including the dataset characteristics, the computer system used and experimental results. The last section presents the conclusion of this work.

II. RELATED WORK

In [8] authors introduce a framework to detect the semantic changes in the VHR images by removing the false changes. This framework depends on extracting four descriptors (descriptor is considered to be any possible feature can be extracted from the image and can be modelled as a function). The first descriptor is used to generate a map of actual (semantic & false) radiometric changes using the CVA in polar domain. The second descriptor is used to generate the shadow map. The third descriptor is used to generate the registration noise map. The fourth descriptor is used to generate multitempral parcels that are homogeneous in both temporal images. Descriptors extraction is followed by applying the context based fusion to generate semantic change map.

III. PROPOSED FRAMEWORK

The proposed framework aims to enhance the results of using the framework mentioned before. The enhancement takes place only in the first descriptor. The proposed framework can be divided into 3 main stages, Fig. 1. The first stage is a preprocessing step which aims to reduce the false changes by providing geometric and radiometric correction. The second stage is the extraction of four descriptors. The first descriptor is obtained using V_1 (Absolute difference between {red, green, blue and hue} layers) and V_2 (Change vector analysis) that used in generating a map of actual (semantic & false) radiometric changes. Other descriptors are obtained as same as the framework introduce by Lorenzo Bruzzone and Francesca Bovolo in 2013. The third stage aims to generate the final change map by applying the context based fusion between all descriptors that generated in the second stage.

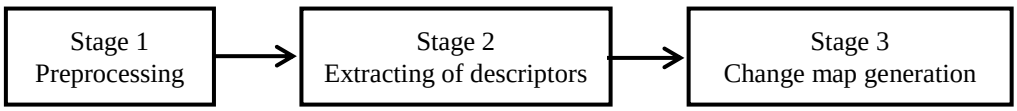

Fig. 1. Stages of applying the proposed framework

IV. EXPERIMENTAL WORK

Two experiments are conducted on two datasets applying the proposed framework. The first experiment is performed to detect the changes between real VHR image and simulated image. The second experiment is performed to detect the changes between two real VHR images.

A. Remote sensing dataset used

Two datasets are used in this paper. The real images are taken by El-Shayal Smart web on Line Software that could acquire Satellite images from Google Earth. The dataset area lies between Lat. 41 53 17.8919 N, Lon. 12 33 14.5522 E and Lat. 41 53 12.9891 N, Lon. 12 33 19.3700 E. The first dataset consists of one real VHR image of Municipio City, Italy acquired at 2007 and one simulated image. The simulated image was generated from the real image by adding some predefined features. The added features provide a reference (ideal) change map, Fig. 2. The added features occupy 34484 changed pixels. These changes are introduced in a way to be seemed as real changes. In particular, the features have been added to the scene taking their geometrical structures and spectral signatures from real features given in different portions of the real image. Table (1) summarizes the characteristic of the first dataset. The second dataset consists of two real VHR images. The first image is of the same area in first dataset, Fig. 3(a). The second image is of the same area acquired at 2011, Fig. 3(b). Table (2) summarizes the characteristics of the second dataset.

ISSN(Online): 2320 - 9801
ISSN (Print) : 2320 - 9798

International Journal of Innovative Research in Computer and Communication Engineering

(An ISO 3297: 2007 Certified Organization)

Vol. 4, Issue 6, June 2016

Table (1): Characteristic of the first dataset

No	Spatial resolution (cm)	Radiometric resolution (bits)	Number of bands	Acquisition date	Size (pixels)
1	50	8	3	2007	983*983
2	50	8	3	Simulated	983*983

(a) (b) (c)

Fig. 2. (a) The real image of Municipio City, Italy acquired at 2007, (b) The similated images of image (a) after adding some predefined features and (c) The reference change map between images (a) and (b) .

Table (2): Characteristic of the second dataset

No	Spatial resolution (cm)	Radiometric resolution (bits)	Number of bands	Acquisition date	Size (pixels)
1	50	8	3	2007	700*700
2	50	8	3	2011	700*700

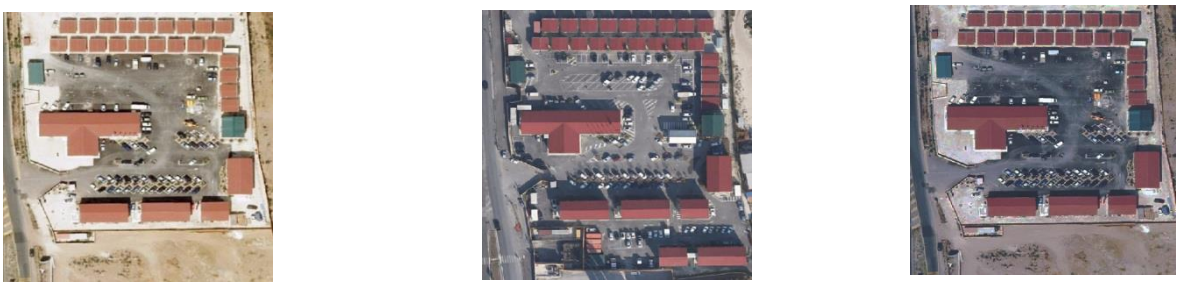

(a) (b) (c)

Fig. 3. Second dataset of Municipio City, Italy acquired at: (a) 2007, (b) 2011 and (c) Image of 2007after applying the histogram matching technique.

B. Computer system used

Hardware: A laptop machine with processor Intel(R)core(TM)i7- 4500U CPU @1.80 GH 2.40 GH and RAM 8 GB is used with windows 7 operating system.

Software packages: MATLABR2014b and ERDAS IMAGINE 2014 software's are used. All the experiment operations are performed using MATLAB except the segmentation process is performed using ERDAS IMAGINE.

C. Experiment steps (Application of the proposed framework)

Fig. 4 shows the detailed block scheme of the three stages of applying the proposed framework.

Stage 1: Preprocessing

In the first experiment there is no need for this stage (because the simulated image is artificially generated without any distortions). In second experiment, a radiometric correction is necessary to reduce the false changes that

ISSN(Online): 2320 - 9801
ISSN (Print) : 2320 - 9798

International Journal of Innovative Research in Computer and Communication Engineering

(An ISO 3297: 2007 Certified Organization)

Vol. 4, Issue 6, June 2016

appear due to the variation in solar illumination conditions, atmospheric conditions, differences in soil moisture and viewing geometry at different acquisition times [1, 15]. In this paper, Histogram matching technique is applied, the results are shown in Fig. 3(c), followed by normalization [8]. A geometric correction is not needed because the dataset had been registered by El-Shayal Smart web on Line Software.

Stage 2: Descriptors extraction

In this stage the problem of shadow and registration noises is solved by removing the false changes that couldn't be removed in the first stage. Four descriptors should be extracted. The first descriptor D_1 is concerned with the detection actual radiometric changes that occurred through the period 2007 to 2011 using V_1 and V_2 separately (the first experiment represents a comparison between them). The second descriptor D_2 is concerned with the shadow detection. The third descriptor D_3 is concerned with the detection of the registration noise. The fourth descriptor D_4 is aimed to generate the multitemporal parcels. The detailed extraction procedures of the four descriptors are given in the following subsections.

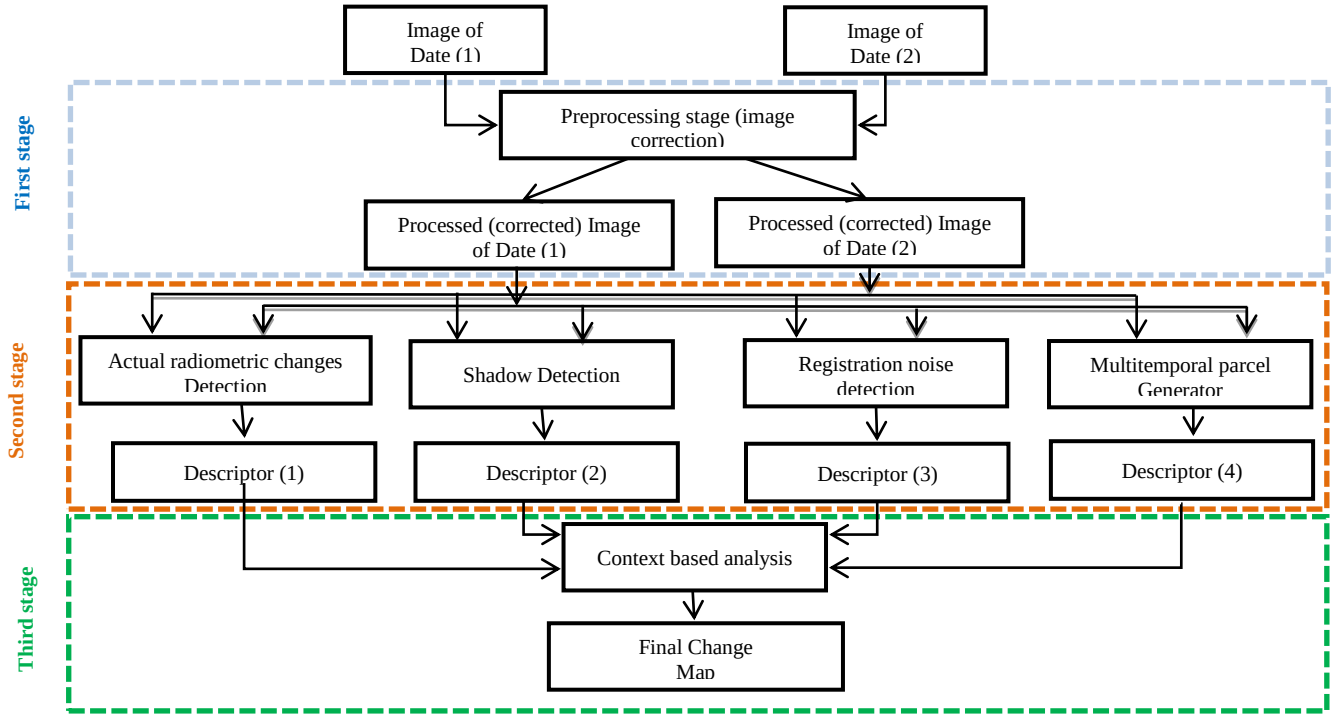

Fig. 4. Detailed block scheme of the change-detection system defined by using the proposed framework for solving the change-detection problem.

- ***Actual radiometric change descriptor D_1***

The map of actual radiometric changes can be obtained by using V_1 (proposed by us) and V_2 (proposed in [8]). The statistical distribution of the results can be modeled as a sum of two distributions associated with the class of non-changed (ω_n) and changed (Ω_c) pixels, respectively. These classes can be separated using expectation maximization (EM) algorithms.

The First Experiment

The actual radiometric change detection maps are obtained by modeling the statistical distributions of the two vectors as a sum of two distributions associated with the class of non-changed (ω_n) and changed (Ω_c) pixels, respectively. V_1 and V_2 are resulted from some kind of subtraction of the layers of the first dataset .So, its distribution can also be reasonably represented as a mixture of multidimensional Gaussian Distributions described by their mean value and variance. This is because the statistical distribution of the natural classes in the image acquired by the multispectral passive sensor can be considered approximately Gaussian [16]. Fig. 5(a) shows plotting the estimated

ISSN(Online): 2320 - 9801
ISSN (Print) : 2320 - 9798

International Journal of Innovative Research in Computer and Communication Engineering

(An ISO 3297: 2007 Certified Organization)

Vol. 4, Issue 6, June 2016

probability density contours for the two-component mixture distribution (ρ and θ of applying V_2). The two bivariate normal components overlap, but their peaks are distinct. This suggests that the data could reasonably be divided into two classes [16]**.** To separate the two classes, The Bayesian decision rule for minimum error is applied according to [17]. Statistical class parameters have been estimated by the unsupervised method presented in [17] based on the expectation–maximization algorithm [18]. This operation leads to the generation of a binary map that separates radiometrically changed pixels, white color, from the unchanged pixels, black color, as shown in Fig. 5(b, c). The superiority of using V_1 over V_2 was validated objectively and subjectively as illustrated in Table (3) and Fig. 5(b, c).

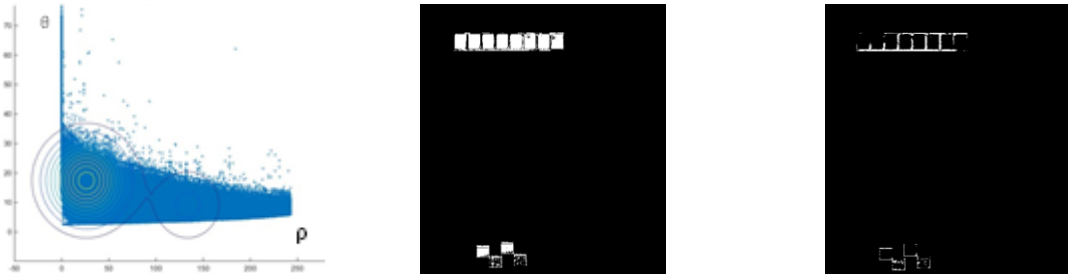

(a) (b) (c)

Fig. 5. (a) Probability density contours for the two-component. (b) Actual radiometric change maps obtained by using V_1. (c) Actual radiometric change maps obtained by using V_2.

Table (3): actual radiometric change map results obtained on the first dataset

	Absolute difference with hue (V_1) (proposed)	CVA (V_2) (given in [8])
Total changed pixel	34484	34484
Resulted changed pixel	25110	6448
Missed alarm	9374	28036
Degree of success (%)	72.81 %	18.69 %

The Second Experiment

Fig. 6 illustrates the results obtained after applying V_1 , Fig. 6(a), and applying V_2 , Fig. 6(b), on the second dataset.

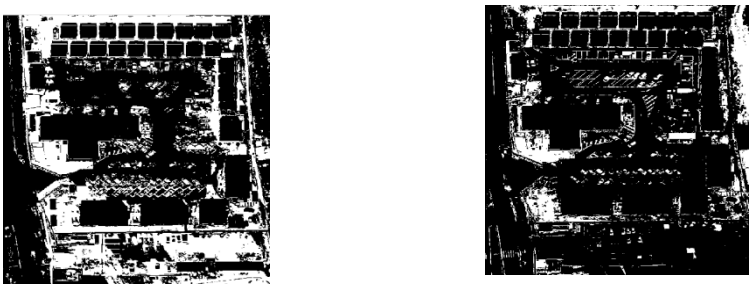

(a) (b)

Fig. 6. Actual radiometric change maps obtained from using V_1 (a) and V_2 (b)

- ***Shadow descriptor D_2***

The shadow descriptor can be calculated by subtracting the shadow indices ($shad$) of the second dataset as follow:

$$\boldsymbol{D_2} = shad_2 - shad_1$$

For more details in shadow indices calculation see [19]. D_2 can be modeled as a sum of two statistical distributions associated with shadow or non-shadow classes [8]. A binary map was generated to separate shadow class, white color, from non-shadow class, black color, as shown in Fig. 7.

ISSN(Online): 2320 - 9801
ISSN (Print) : 2320 - 9798

International Journal of Innovative Research in Computer and Communication Engineering

(An ISO 3297: 2007 Certified Organization)

Vol. 4, Issue 6, June 2016

- ***Registration noise descriptor: D_3***

Reducing the resolution of images leads to decrease the impact of the registration noise with respect to that on the original scene, of full resolution, as shown in Fig. 8. Spectral change vectors (SCVs) associated with RN {dashed circles in Fig. 8(a)} tends to disappear collapsing into, while the cluster of pixels associated with true changes {region marked with continuous circles in Fig. 8(b)} reduces its spread.

Fig. 7. Binary shadow map. Shadow effect is in white area while non-shadow is in black area.

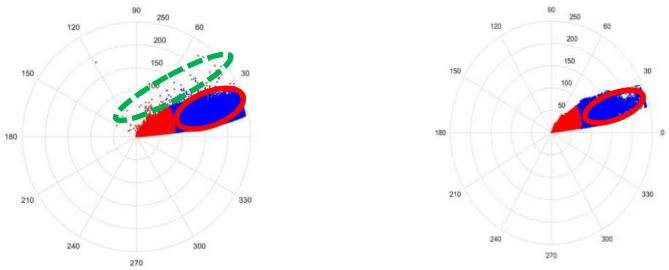

(a) (b)

Fig. 8. Polar coordinate system obtained by applying the CVA technique at (a) full resolution and (b) one-eight resolution

It is worth noting that, the choice of the cell size can significantly affect the performance of identification the registration noise. So, seven levels of decomposition aim to overcome this problem by exploiting different cell size followed by applying the majority voting rule levels for each cell to provide an adaptive identification of the final registration noise map. For more details in registration noise identification see [9].

- ***Multitemporal parcel generation : D_4***

The multitemporal parcel is generated by ERDAS IMAGINE 2014 software. Stack layers tool box was used to stack all layers of the two images to generate one image then image segmentation tool in ERDAS IMAGINE 2014 software is used to generate a segmented image. This descriptor allows distinguishing between the changed and non-changed areas. As the changed areas should have different characteristics compared with non-changed areas.

Stage 3: generation of final change map based on Context-sensitive analysis

Once noise sources have been identified, they can be removed from the map of radiometric changes according to a context-based implementation of the fusion strategy as shown in Fig. 9. For more details about fusion strategy see [8].

D. Overall accuracy assessment of the final change map

The change error matrix (the confusion matrix) is produced using 100 random points. The reference information has been taken visually by comparing the two real images. Table (4) illustrates the confusion matrices which obtained from applying the proposed framework using V_1 and V_2 respectively on the second dataset. Using V_1 in the proposed

ISSN(Online): 2320 - 9801
ISSN (Print) : 2320 - 9798

International Journal of Innovative Research in Computer and Communication Engineering

(An ISO 3297: 2007 Certified Organization)

Vol. 4, Issue 6, June 2016

framework shows its superiority over using V_2 by providing highest overall accuracy 83% while V_2 provides 74% as shown in table (5). Detailed calculation of accuracy assessment is given in [1].

(a) (b)

Fig. 9. Final change maps obtained from using V_1 (a) and V_2 (b)

Table (4): The change error matrix of the final change image map obtained from applying the proposed framework using V_1 and V_2 on the second dataset.

Classified data	**Reference data**					
	Change		No Change		Total	
	V_1	V_2	V_1	V_2	V_1	V_2
Change	13	6	7	9	20	15
No Change	10	17	70	68	80	85
Total	23	23	77	77	100	100

Table (5): Final change detection map results obtained on the second dataset

	Framework given in [8]	Proposed framework
Total pixels	490000	490000
Resulted changed pixels	51016	89025
Changed area	10.41%	18.16 %
Overall accuracy (%)	74 %	83 %

V. CONCLUSION

The CD from RS data is affected by various elements, including spatial, spectral, temporal, radiometric resolution, atmospheric conditions, and soil moisture conditions. Many techniques have been developed for addressing the CD problems, especially for moderate and high resolution images. However, these methods are ineffective when dealing with very VHR images. Increasing geometrical resolution requires developing new techniques to keep pace with the resolution increasing. Especially, most of the classical CD techniques assume spatial independence among pixels, which is not reasonable in VHR images. This paper presents an enhanced framework for CD in VHR remote sensing multitemporal images. It is based on the spatial context information of multitemporal adaptive regions homogeneous both in spatial and temporal domain (parcels) for detecting the semantic changes by excluding the shadow and the misregistration noises. These parcels exploit the spatial correlation among neighboring pixels which allow getting accurate and reliable CD maps by integrating the spectral information with the spatial one and modeling the multiscale properties of the scene. The qualitative and quantitative analysis of the results obtained on two dataset made up of a simulated and a real images of Municipio City in Italy point out that the proposed framework involves a

ISSN(Online): 2320 - 9801
ISSN (Print) : 2320 - 9798

International Journal of Innovative Research in Computer and Communication Engineering

(An ISO 3297: 2007 Certified Organization)

Vol. 4, Issue 6, June 2016

low amount of false alarms in CD maps. In more detail, the achieved results from the simulated dataset indicates the superiority of using absolute difference between {red, green, blue and hue} layers as a vector (V_1) in the proposed framework over using CVA as a vector (V_2). Using V_1 in the proposed framework provides overall accuracy 83 % and indicating that 18.16 % of the image area had been changed over the period from 2007 to 2011while, using V_2 in the given in [8] provides overall accuracy 74 % and indicating that 10.41% had been changed. The proposed framework shows its validation when dealing with dataset of little difference in shooting angles. This makes the effect of shadow and registration noises to be small for low-height objects compared with great-height objects.

REFERENCES

1. Mostafa Mosaad, A.H., Mahmoud Safwat and Fawzy Eltohamy Detection of the urban expansion over agricultural land using LULC change detection techniques:case study El-Mahalla el-koubra City-Egypt. International Journal in IT and Engineering, **3**(11,.2015.
2. Chen, G., et al., Object-based change detection. International Journal of Remote Sensing, **33**(14): p. 4434-4457, 2012.
3. Singh, A., Review article digital change detection techniques using remotely-sensed data. International Journal of Remote Sensing, **10**(6): p. 989-1003, 1989.
4. Hussain, M., et al., Change detection from remotely sensed images: From pixel-based to object-based approaches. ISPRS Journal of Photogrammetry and Remote Sensing, **80**: p. 91-106, 2013.
5. Lu, D., et al., Change detection techniques. International Journal of Remote Sensing, **25**(12): p. 2365-2401m, 2004.
6. Jianya, G., et al., A review of multi-temporal remote sensing data change detection algorithms. The International Archives of the Photogrammetry, Remote Sensing and Spatial Information Sciences, **37**(B7): p. 757-762, 2008.
7. Al-doski, J., S.B. Mansor, and H.Z.M. Shafri, Change Detection Process and Techniques. Change, **3**(10), 2013.
8. Bruzzone, L. and F. Bovolo, A novel framework for the design of change-detection systems for very-high-resolution remote sensing images. Proceedings of the IEEE, **101**(3): p. 609-630, 2013.
9. Marchesi, S., F. Bovolo, and L. Bruzzone, A context-sensitive technique robust to registration noise for change detection in VHR multispectral images. Image Processing, IEEE Transactions on, **19**(7): p. 1877-1889, 2010.
10. Dewidar, K.M., Detection of land use/land cover changes for the northern part of the Nile delta (Burullus region), Egypt. International Journal of Remote Sensing, **25**(20): p. 4079-4089, 2004.
11. Pacifici, F. and F. Del Frate, Automatic change detection in very high resolution images with pulse-coupled neural networks. Geoscience and Remote Sensing Letters, IEEE, **7**(1): p. 58-62, 2010.
12. Ru, H., et al. Superparsing based change detection in high resolution remote sensing imagery. in Signal Processing (ICSP), 2014 12th International Conference on. IEEE. 2014.
13. Huang, X., L. Zhang, and T. Zhu, Building change detection from multitemporal high-resolution remotely sensed images based on a morphological building index. Selected Topics in Applied Earth Observations and Remote Sensing, IEEE Journal of, 2014. **7**(1): p. 105-115.
14. Vakalopoulou, M., et al. Simultaneous registration and change detection in multitemporal, very high resolution remote sensing data. in Proceedings of the IEEE Conference on Computer Vision and Pattern Recognition Workshops. 2015.
15. Deer, P., Digital change detection techniques in remote sensing. 1995.
16. MATLABR2014b, help of Fit Gaussian mixture distribution to data. 2014.
17. Bruzzone, L. and D.F. Prieto, Automatic analysis of the difference image for unsupervised change detection. Geoscience and Remote Sensing, IEEE Transactions on, **38**(3): p. 1171-1182, 2000.
18. RichardsJA, J., RemotesensingDigitalImageAnalysis: AnIntroduction, Berlin: springer, 1999.
19. Huang, J., W. Xie, and L. Tang. Detection of and compensation for shadows in colored urban aerial images. in Intelligent Control and Automation, WCICA 2004. Fifth World Congress on. 2004. IEEE, 2004.